Theoretical and Simulated Capacity of Urban Air Mobility Airspace Characteristics

Casey L. Denham *, William G. Cummings†, and Jeremy C. Smith ‡
NASA Langley Research Center, Hampton, VA 23681

As interest in urban air mobility grows, so are the optimistic predictions for potentially hundreds of simultaneous operations within a given metropolitan airspace. This high density of traffic poses a challenge for safe, efficient, and timely operations, particularly when realistic airspace restrictions, fleet sizes, and fluctuating demand are considered. Routes for urban air mobility aircraft, similar to automotive roadways more than other types of airways, are one proposed solution for traffic management. This paper identifies several potential components of urban air mobility routes and compares their numerically predicted maximum capacity with what is achieved in a realistic simulation that includes airspace restrictions, parking limitations, fleet sizes, and uneven demand.

Nomenclature

δ	=	capacity, aircraft/hr
θ	=	intersection angle, deg
d	=	diameter of circular portion of rotary intersection
e	=	number of entrances for rotary intersection; assumed equivalent to number of exits
v	=	aircraft velocity, kts
r	=	aircraft separation standard, ft

I. Introduction

As progress is made towards the start of Urban Air Mobility (UAM) operations, it is important to anticipate issues that may arise as the quantity of operations grows. Some of these issues are societal, such as the acceptance of travel using smaller, potentially unmanned aircraft, or related to the business case, such as the anticipated demand dependent on the cost of travel. However, many potential issues have to do with how these vehicles operate and the rules and procedures that govern them.

NASA's Air Traffic Management - eXploration (ATM-X) project aims to address these challenges faced by the entrance of UAM operations into the National Airspace System through focused research [1]. In particular, the UAM subproject focuses on the technologies and architectures for airspace and vertiport management that will enable widespread UAM operation [1, 2]. Research goals include safe mission planning and operation, separation assurance, dynamic scheduling, congestion management, and interoperability with other air traffic [1]. The research described in this paper was conducted to better understand congestion management, particularly investigating the relationship between various features of a purpose-designed airspace and their impact on the maximum safe capacity.

Others have previously studied the constraining factors with regards to airspace capacity in the commercial aviation and small Unmanned Aerial System (sUAS) sectors. Xue describes the use of corridors in the sky or "tubes" to reduce controller workload and increase the capacity possible in a given airspace and then expands the study to the fuel requirements and complexity changes associated with this concept [3, 4]. A method utilizing a non-dominated sorting genetic algorithm (NSGA) to reduce the amount of delay experienced due to scheduling in terminal airspace is also proposed, and a fast time simulation tool capable of modeling sUAS operations to test the impact of various parameters, rules, and models, and evaluate them statistically in realistic environments was created created [5, 6]. More specifically to UAM applications, Mueller et al. described the barriers to integrating UAM services within the National Airspace

*Aerospace Technologist - Aerospace Vehicle Design and Mission Analysis, Aeronautics Systems Analysis Branch, MS 442
†Aerospace Technologist - Aerospace Vehicle Design and Mission Analysis, Aeronautics Systems Analysis Branch, MS 442
‡Aerospace Technologist - Aerospace Flight Systems, Aeronautics Systems Analysis Branch, MS 442

System (NAS) and offered a roadmap for expanding the framework developed for sUAS Traffic Management (UTM) to UAM applications [7]. Vascik et al. focused on the integration of UAM with existing air traffic through geometric airspace design [8].

The analysis in this paper assumes a baseline quantity and demand distribution typical of UAM Maturity Level 4 (UML-4) operations. UMLs detail the progression of UAM operations within the NAS, from pre-operational to ubiquitous and widespread use [9–11]. UML-4 operations are defined by medium traffic density on the order of hundreds of simultaneous operations, substantial flight and contingency management automation, and the potential for remotely piloted vehicles [9, 10]. Separation standards used in this analysis are notional values that may be updated based on a rigorous safety case in the future. The system level impact on demand was studied in our companion paper, Cummings et al., and applies the concepts discussed in this paper to a metropolitan area scale system.

The Airspace Routing, Conflict, and Scheduling Simulation (ARCSS) analysis tool that was created to support this work is described in Section II. Section III describes the mathematical method that was used to calculate the maximum capacity of airspace design features under ideal circumstances. These features start with simple corridors and intersections then expand to include more complex structures. Section IV explains the method through which these features are combined into an airspace design, as well as comparison with the simulated capacity for the same system. Finally, Section VI contains a summary and conclusions, as well as recommendations for future work.

II. Airspace Routing, Conflict, and Scheduling Simulation (ARCSS) Tool

The Airspace Routing, Conflict, and Scheduling Simulation, or ARCSS, is a new tool that was developed in MATLAB® for this project. It enables quick simulation and evaluation of airspace route structures, conflict resolutions, and scheduling protocols. It is similar to other mission planners that also use a pre-planning approach to detect and resolve conflicts before determining an aircraft's trajectory, however ARCSS is designed to quickly and easily modify airspace and route structures [13]. This pre-flight approach enables testing of conflict avoidance strategies without requiring a high fidelity simulation of the aircraft dynamics or substantial computational power.

By using an object-oriented approach, airspace characteristics including vertiports, routes, airspace constraints, and aircraft were able to be defined in a generic manner with default values that were then able to be modified to accommodate a wide spectrum. An example of this is with vehicle types, where a UAM aircraft is defined with preset values for speed, horizontal separation standard, and maximum altitude, but each of these values is able to be independently changed for a given aircraft. Figure 1 shows an example from a typical ARCSS simulation, including vertiports, airspace constraints, UAM vehicles, and the conflict notification bar, which details information about any predicted loss of separation between aircraft or intrusion of airspace constraints.

ARCSS includes conflict detection functionality that enables identification of instances of predicted loss of separation or violation of airspace constraints, as well as simple conflict resolution strategies. Currently the primary conflict resolution method is adding an on-ground departure delay but other strategies, such as altitude changes, horizontal trajectory changes, or velocity changes, are also possible.

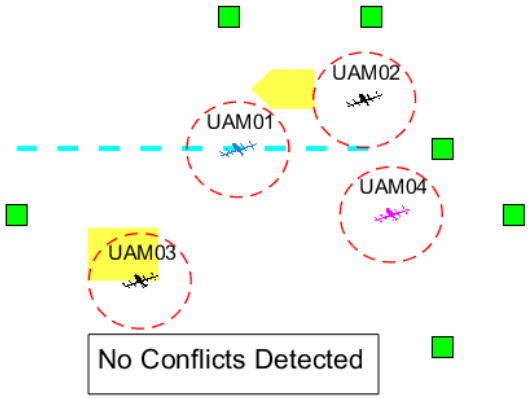


Fig. 1 Screenshot of ARCSS, including vertiports (green squares), airspace constraints (yellow shaded region), defined route (cyan dashed line), UAM aircraft, and conflict notification bar.

III. Definition of Airspace Characteristics and Theoretical Capacity

To calculate the theoretical maximum capacity of an airspace characteristic, a volumetric flow approach was used - determining the maximum number of aircraft that could traverse a given volume within a set amount of time. For this initial analysis, it is assumed that all the aircraft in the simulation have the same constant velocity. For intersections, it is also assumed that the aircraft on each route alternate passing through the intersection. This approach gives a best-case estimate since in a realistic case, the aircraft would not necessarily have the same density, particularly along different routes. However, it is still a useful metric to determine which types of airspace characteristics have the best potential at increasing the overall capacity of the airspace while minimizing conflict, delays, or flight cancellations. For this analysis, all intersection types are assumed to be two dimensional, not relying on the availability of altitude to separate traffic.

The most basic airspace route characteristic is a simple, one-directional route. An example of this geometry is shown in Fig. 2, where an aircraft travels along a route, passing through a control volume, indicated by the blue shaded region. The maximum capacity of this feature can be defined using

$$\delta^{\text{simple route}} = \frac{v}{r} \tag{1}$$

where v is the aircraft velocity, and r is the radius of the horizontal separation standard. For the default case, with aircraft speed of 120 kts and a notional horizontal separation standard of 1200 ft, this results in a capacity, $\delta^{\text{simple route}}$ of 600 aircraft/hr. Simple routes are often used to direct traffic around a constraint or to reduce the workload of managing many aircraft. While one-directional routes do have the greatest capacity, it would be impractical to construct an entire airspace network out of only one-directional routes without any intersections.

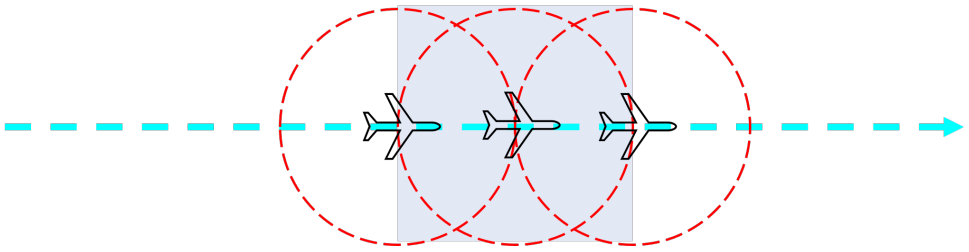


Fig. 2 Depiction of a simple route, with one directional travel, showing an aircraft traversing the control volume.

A two-directional single lane route, where aircraft can travel in either direction along the same route, introduces substantial delays and requires lateral or vertical deconfliction to be a robust route component. Because traffic can only flow in one direction at a time, an aircraft traveling in the opposite direction must wait until the original aircraft has traversed the entire route. Depending on the length of the route, this effectively reduces the capacity to near zero. For this reason, two-directional routes are not considered for this work. If two-directional flow is needed, parallel routes are required.

A. Perpendicular Intersection

In terms of capacity, the most straightforward intersection is one with two perpendicular directions of travel. An example intersection is shown in Fig. 3, where routes A and B intersect at a right angle. Using the previously noted assumption of alternating traffic, only minimal aircraft delays are required to resolve the airspace conflicts. The capacity for a single route of the intersection, route A, can be written using:

$$\delta^{\text{simple intersection}} = \frac{v}{\sqrt{2r^2}} \tag{2}$$

resulting in a capacity $\delta^{\text{simple intersection}}$ of 424 aircraft/hr for the default case. However, it is not always practical to have every intersection in an airspace intersect perpendicularly, so other types of intersections are required.

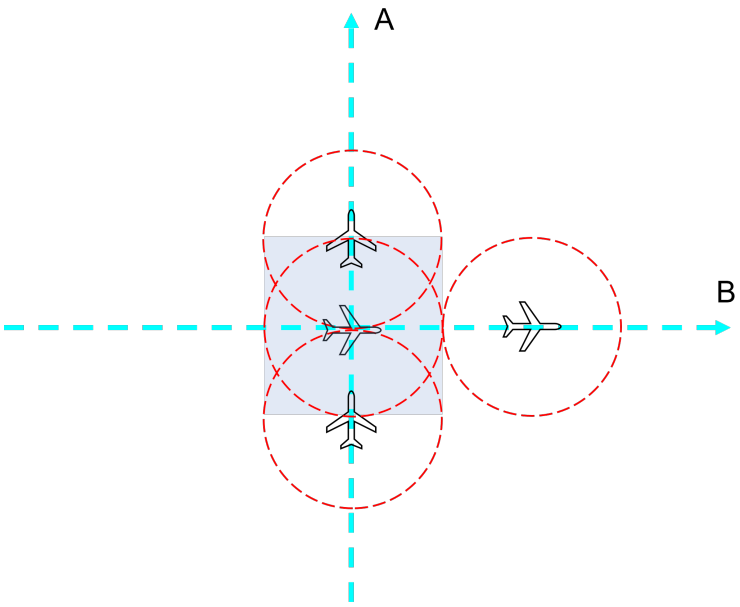


Fig. 3 Depiction of a simple intersection, with two perpendicular directions of travel, showing two aircraft traversing the control volume.

B. Angular Intersection

For the case of two routes which do not intersect perpendicularly, an example of which is shown in Fig. 4, the capacity depends on the angle of intersection, θ. The mathematically derived capacity, $\delta^{\text{angular intersection}}$, is defined as:

$$\delta^{\text{angular intersection}} = \frac{v}{\frac{r}{\sin((180^\circ - \theta)/2)}} \tag{3}$$

This type of intersection can have differing capacity, varying from that of a single directional route to zero flights per hour. Figure 5 illustrates this capacity as a function of intersection angle. This information can be used to design intersections which conform to the physical layout of the airspace, but can also meet the required demand.

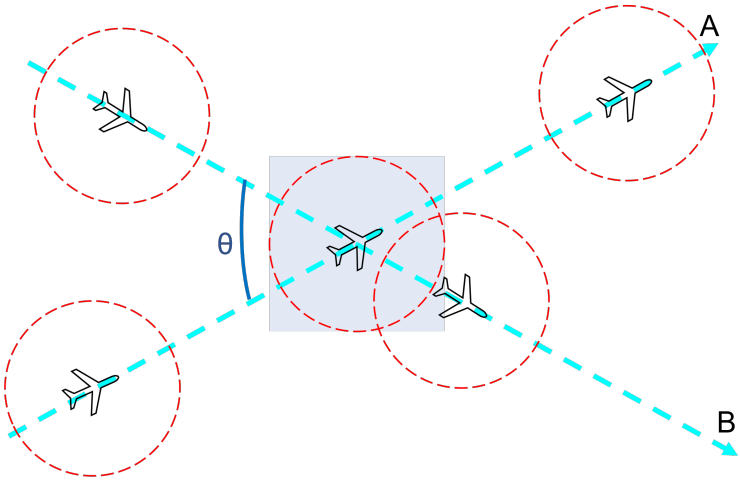


Fig. 4 Depiction of an intersection with two directions of travel offset by angle θ, showing two aircraft traversing the control volume.

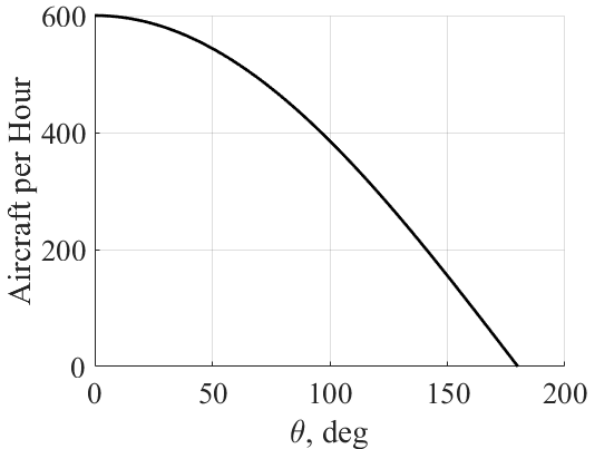
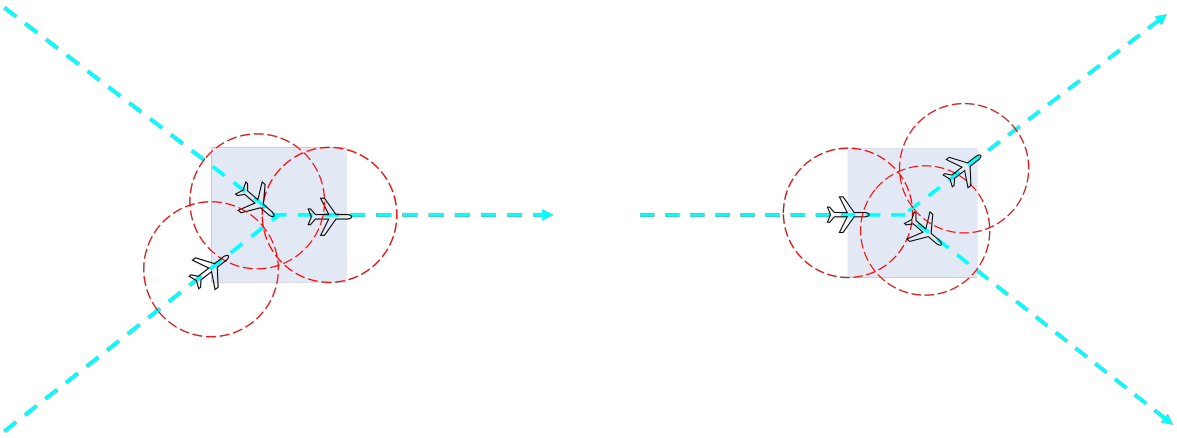


Fig. 5 Effect of intersection angle on the capacity of the intersection, with acute angles having larger capacity and larger angles causing substantial reduction.

C. Converging and Diverging Intersections

Although converging and diverging intersections, shown in Figs. 6a and 6b, may appear to be quite different at first glance, the capacity of both is limited by the single route portion of the intersection, using the assumption of an aircraft with constant speed and that the combined route is no less that 90° from either of the single routes. These are important components for building more complex airspace routing structures, particularly since not every flight will have the same start or end location along the route, but it is still possible to condense them into a single route without introducing additional delays.



(a) Converging Intersection **(b) Diverging Intersection**

Fig. 6 Depiction of intersections with converging and diverging routes offset by angle θ.

D. Rotary Intersection

Rotary intersections, also known as roundabouts or traffic circles, are widely used in automotive routes, but might be suitable to use in an airspace route structure. One benefit to such an intersection is the continuous flow of traffic, particularly when future advanced air mobility aircraft may or may not be able to hover and "stop". Figure 7 shows an example rotary intersection, which contains three pairs of on and off ramps along the circular route. This type of intersection can be thought of as a combination of the other route elements previously discussed - a simple one-directional route for the circular portion, converging intersections for the on ramps, and diverging intersections for the off ramps. By building up complex route structures using these basic elements, the capacity can easily be calculated. In the case of

a rotary intersection, because the subcomponents all have a maximum capacity equivalent to a one-directional route, the circumference of the circular portion drives the capacity. For example, a rotary intersection with a radius of 5000 ft can accommodate 26 aircraft in the circular portion at a single time, using the default assumption of a 1200 ft horizontal separation standard. Additional aircraft must wait until an aircraft exits the intersection and the resulting gap cycles back to their entrance point, introducing substantial delay. Using the assumption that, on average, the flights are randomly distributed and therefore the average aircraft will travel half of the circular portion, the additional delay added can be estimated, shown mathematically in Eq. 4. Note that this capacity limit does not depend on the size of the rotary intersection or the number of entrances and exits. For the 5000 ft radius rotary intersection with the default speed and separation standards, the maximum capacity is 1200 aircraft per hour. Even though the capacity does not change with size, it is important that rotary intersections be sized to accommodate the number of aircraft expected to simultaneously use the intersection, while keeping in mind that excessive size will result in longer flight times for all aircraft.

$$\begin{aligned} \delta^{rotary} &= \frac{1}{\text{Average Time in Circle}} * \text{Capacity of Circular Portion} \\ \delta^{rotary} &= \frac{1}{\frac{0.5\pi d}{v}} \frac{\pi d}{r} = \frac{2v}{r} \end{aligned} \tag{4}$$

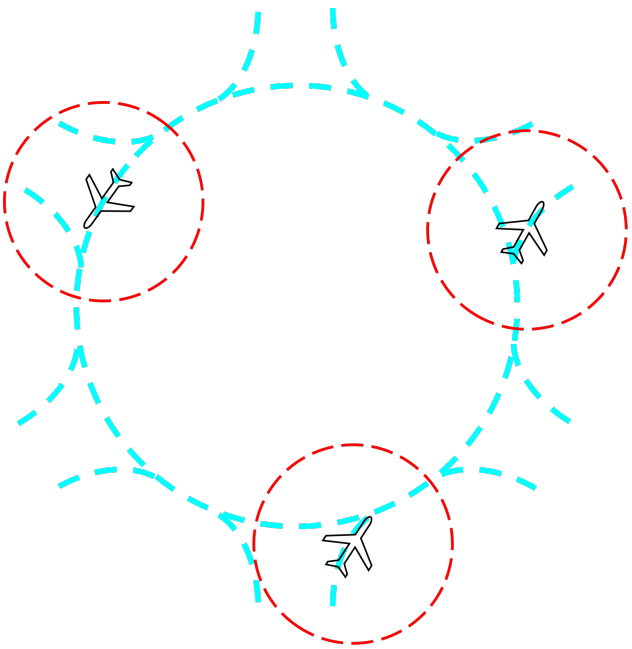


Fig. 7 A roundabout structure, with on and off ramps for aircraft.

IV. Comparison of Theoretical Capacity to Simulated Capacity

For each of the intersection types detailed above, the capacity will be simulated for the worst-case, alternating case used to calculate the mathematical limits, a randomized, but equal, demand case, and a weighted demand case, where each route and vertiport has different demand. For these simulations, vertiport takeoff timing was not considered, so that flights could begin as soon as the route was clear. This assumption allows a calculation of the maximum capacity along the route which is unaffected by the required time to load and allow each aircraft to take-off. In addition, the delay and maximum capacity are heavily impacted by the time step used for the simulation. For this analysis, the time step was set as 0.01 minute, which does cause small increases to the delay and reduces the maximum capacity, but is sufficiently accurate enough for this study.

A. Perpendicular Intersection - Simulated

For the perpendicular intersection, the worst-case alternating scenario results in a maximum capacity of 413 flights per hour. While this is slightly higher than the theoretical calculation, this is due to the time step selection. As expected, the random and weighted scenarios show an increase in the maximum capacity, with an increase of approximately 17% in the random scenario, and 24% in the weighted case. The large increase for the weighted case indicates that perpendicular intersections may be a suitable choice when it is expected that one route will have a much higher demand than the other.

B. Angular Intersection - Simulated

To simulate the range of potential angular intersections, angles of 15°, 30°, 45°, 60°, 120°, 135°, 150°, and 165° were used, demonstrating the effect of intersection angle on capacity. A summary of these results compared to the theoretical maximum is shown in Fig. 8, where the red stars indicate the alternating scenario, the blue squares indicate the random scenario, and the green triangles indicate the weighted scenario, and the black line the theoretical maximum as calculated using Eq. 3. For the smaller intersection angles under 45°, the simulation results are slightly below the theoretical maximum because of the time step selection discussed previously. However, for large intersection angles over 90°, the random and weighted cases show significant improvement over the theoretical and alternating cases, due to the large delay required when switching between routes, but these cases remain far below the capacity for a perpendicular intersection. To maximize overall capacity, intersections with smaller intersection angles should be used and routes adjusted to match the origination and destination points.

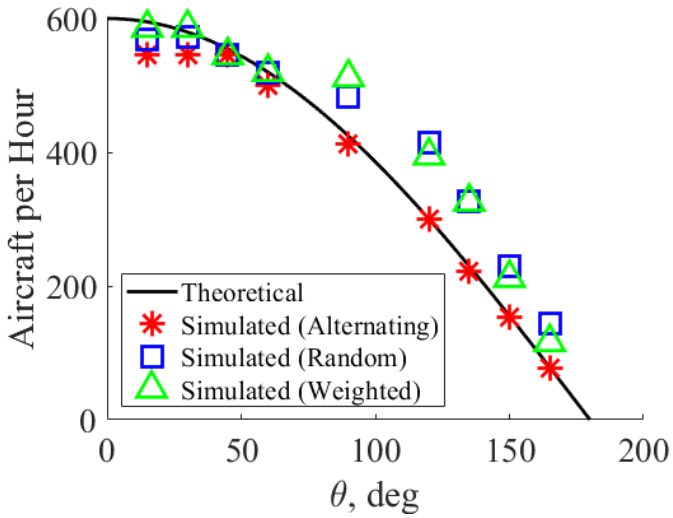


Fig. 8 Comparison showing of intersection angle on the capacity of the intersection, for the theoretical (line), alternating (star), random (square), and weighted (triangle) scenarios. Due to time step resolution, simulated values are lower than the theoretical maximum at acute angles, but both random and weighted show improvement at larger angles.

C. Converging and Diverging Intersections - Simulated

Although all acute converging and diverging intersections are limited by the single directional route in theory, when simulated the maximum capacity is slightly affected by the intersection angle. For the converging intersection, very small angles, such as 15°, have maximum capacity of 550 aircraft per hour, while larger angles, such as 60°, have a maximum capacity of 545 aircraft per hour. The same results are seen in the diverging intersection. Because this difference is relatively small (approximately 10%) and the capacity does not change for the alternating, random, or weighted scenarios, time step refinement was performed to confirm that the decrease in maximum capacity is due to time step size. Having nearly identical capacity for each of the simulation scenarios indicates that it is much easier to estimate the capacity for converging and diverging intersections in the early planning stages, when information about the distribution of flights is not known, as well as intersections where the demand is highly variable throughout the day.

D. Rotary Intersection - Simulated

Because the capacity for a rotary intersection is not affected by the size of the intersection or number of entrances, there is more consistency and predictability to the delay and in turn the capacity, creating a bound to the capacity independent of the number of vertiports. Figure 9 illustrates this - the simulation scenario with alternating demand and every aircraft flying exactly 1/2 of the circle, shown in blue, has some additional delay in departure time (due to time step resolution) compared to the theoretical case with 6 vertiports, but the overall behavior is similar, with large groupings of aircraft with only small delays separated by larger delays in departure time. When looking at the the random demand case, shown in green, although the strong pattern is no longer present, the overall trend of the capacity is close to the alternating case. However, much different behavior is seen in the weighted demand scenario, where 2/3 of the demand starts at the same vertiport, as shown with the magenta line. In this case, the demand from that shared start point overwhelms the remaining demand, and drives the demand capacity towards that of a single one directional route.

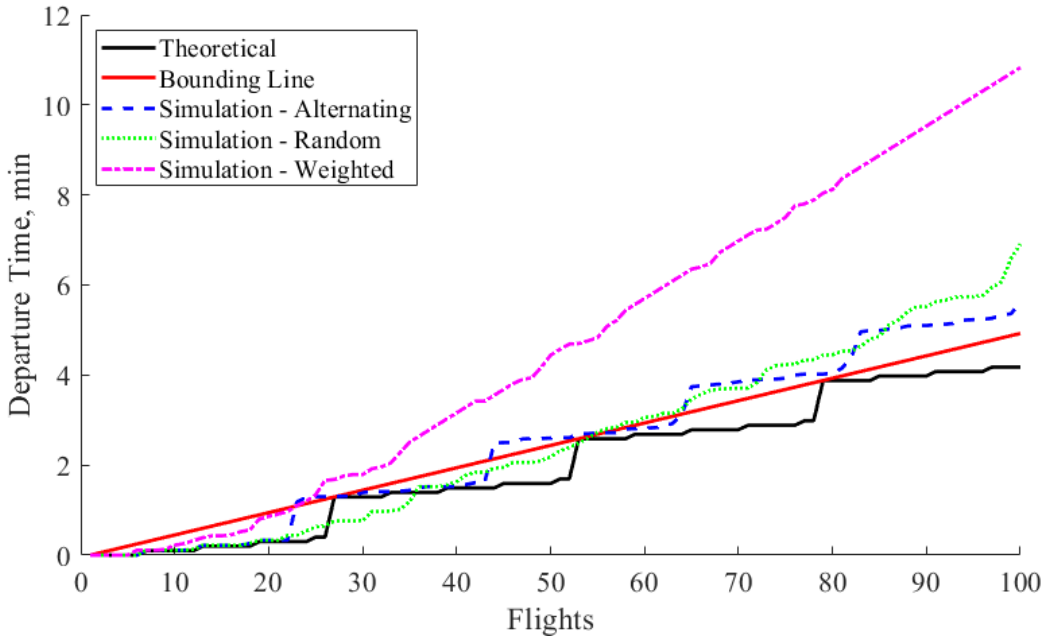


Fig. 9 Comparison showing effect of demand scenarios for the rotary intersection compared to the theoretical case for 6 vertiports in black and the bounding line, calculated using Eq. 4, in red. The alternating, half-circle approximation, shown in blue, has similar behavior to the theoretical case, but the scenario of a heavily weighted demand, shown in magenta, the rotary intersection is unable to keep up with the high demand.

As mentioned in Section III.D, although the capacity for a rotary intersection does not depend on the size, the total flight time certainly does. A larger intersection may allow aircraft to enter more quickly without delay, but they will have a much longer travel time due to the extended route. In some cases, this can mean that the longer travel time counteracts the potential for reduction in delay, with a later arrival to the destination.

E. Summary of Comparison to Theoretical Capacity

As discussed in the previous sections, there are many factors which impact the ability of an airspace feature to reach the theoretical capacity limit, including the weighting of the demand between different routes. Table 1 shows that simple intersections, whether perpendicular or angular, generally perform better when the demand is weighted on one particular route. This is important because it allows for intersections with smaller demand routes without significantly impacting the capacity of the larger route. Conversely, rotary intersections have decreased performance when demand is heavily weighted to one origination point or route, but still offer improvement over the number of intersections they replace.

Feature	Theoretical	Simulated (Alternating)	Simulated (Random)	Simulated (Weighted)
Simple Route	600	600	–	–
Perpendicular Intersection	424	413	482	512
Angular Intersection (30 deg)	579	545	573	586
Angular Intersection (120 deg)	300	300	414	395
Converging Intersection (60 deg)	600	550	550	550
Diverging Intersection	600	550	550	550
Traffic Circle (10k ft diameter)	1200	1133	859	639

Table 1 Comparison of the theoretical and simulated capacity limits for different airspace features.

V. Combining Simple Airspace Characteristics to Generate Larger Airspace Networks

Understandably, the National Airspace is more complicated and contains many different types of intersections. Using the knowledge of the capacity of the previously mentioned airspace structures in isolation, a larger airspace can be created and the capacity can be estimated along each route and for the network as a whole. This capacity estimate can then be used to design or modify airspace route structures and other airspace elements, to improve capacity, reduce delay, and reduce canceled flights.

A. Example Airspace Definition

Figure 10 shows an example airspace model, with a number of vertiports, represented by green squares, airspace constraints, represented by yellow polygons, and defined route structures shown by cyan dashed lines. The demand across the different vertiports is not equal - some vertiports, such as VP01, have a large amount of incoming and outgoing traffic, while some vertiports only have outgoing traffic. This weighting was selected to generate a scenario that may be similar to a downtown region during the morning rush hour, where the majority of the traffic is concentrated within a subset of the total vertiports. The vertiport pairs along with their relative weights, are shown in Table 2. Note that only the VP01-VP03 and VP01-VP05 pairs utilize routes in this scenario, while all other pairs operate on direct path trajectories. This route selection was chosen to demonstrate a strategic deconfliction between the traffic from these pairs and the VP05-VP01 traffic.

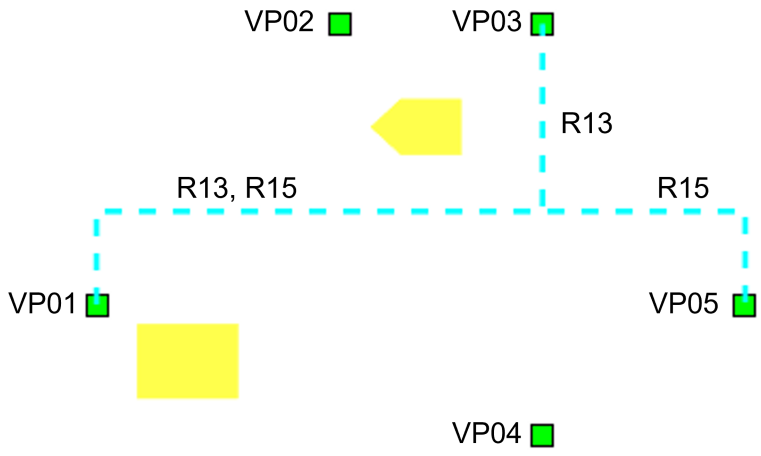


Fig. 10 Example airspace definition, which includes five vertiports represented by green squares, two routes indicated by cyan dashed lines, and two airspace constraint areas represented by yellow polygons.

B. Estimating Route and Overall Capacity

Estimating the capacity of a given airspace first begins with estimating the capacity for each vertiport pair. For the sake of brevity, the process is detailed for a single pair, VP01-VP03, but the process is identical for the remaining pairs. The first step is to isolate the trajectory that traffic for the selected pair will travel and to identify any intersections with other traffic. Because vertiport pairs without a defined route travel a direct trajectory, we can represent those trajectories as pseudo routes. Figure 11 shows this isolation for the VP01-VP03 vertiport pair, with the trajectory for that pair shown in cyan, along with intersecting trajectories for VP02-VP01 (purple), VP01-VP05 (pink), and VP04-VP03 (dark blue).

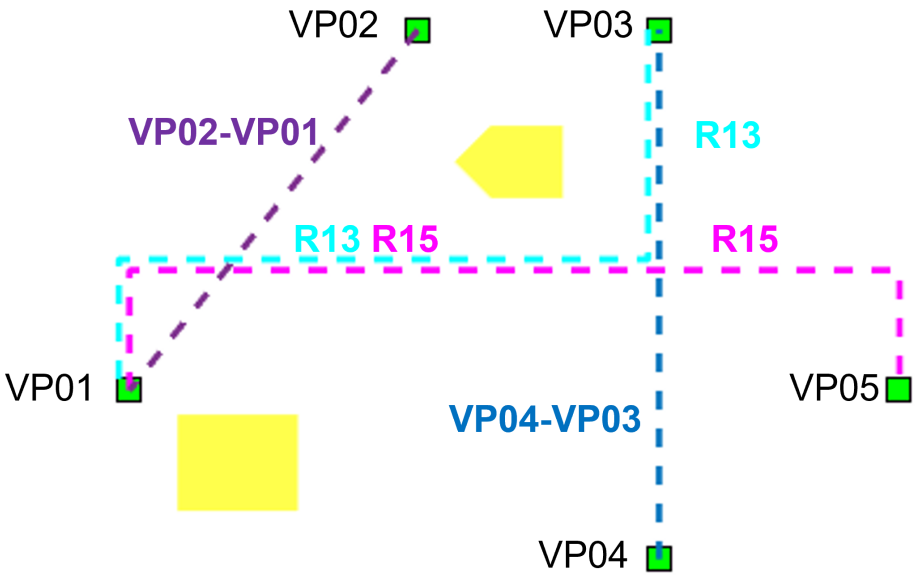


Fig. 11 Isolation of the VP01-VP03 vertiport pair trajectory, shown in cyan, with intersecting routes, R15 (pink), VP02-VP01 (purple), and VP04-VP03 (blue). Note that VP04-VP01 and VP05-VP01 are not shown because they do not intersect the trajectory of interest.

The first intersection we will consider is the angular intersection between VP01-VP03/VP01-VP05 and VP02-VP01 - this is approximately a 120° intersection, therefore the capacity for all routes in the intersection is approximately 300 flights/hour. Because of the alternating traffic assumption discussed in Section III, the estimation results in 150 flights/hour in each direction. However, since two trajectories, VP01-VP03 and VP01-VP05, share the same route at this point, the final result is 92 flights/hour along the VP01-VP03 trajectory, 58 flights/hour along the VP01-VP05 trajectory, and 150 flights/hour along the VP02-VP01 trajectory for this intersection.

The second intersection for the quasi-perpendicular intersection with trajectories from VP01-VP03, VP01-VP05, and VP04-VP03. For a perpendicular intersection, the capacity of all routes is 424 flights/hour, but since VP01-VP03 and VP01-VP05 diverge at this point, we also need to be aware of the capacity of a diverging intersection at 600 flights/hour. Again, using the alternating trajectories assumption, each direction has a maximum capacity of 212 flights/hour. Because the horizontal direction includes two routes, that value is further split, resulting in a capacity of 130 flights/hour along the VP01-VP03 trajectory and 82 flights/hour along the VP01-VP05 trajectory. It is important to confirm that the segment containing flights from both VP01-VP03 and VP04-VP03 has a total capacity less than the the capacity for a single directional route; in this case, the combined capacity is 294 flights/hour, well below the limit.

With both intersections along the route analyzed, the maximum capacity for the route is the minimum across all intersections. For this example airspace scenario, that results in a maximum capacity of 92 flights/hour along the VP01-VP03 route. This analysis was completed for all of the remaining trajectories and the results are shown below in Table 2. The capacity for the entire airspace is the sum of the capacity along each possible trajectory, resulting in a total airspace capacity of 1324 flights/hour.

C. Simulation of Route and Overall Airspace Capacity

Using the ARCSS tool described above, random flights were generated using the vertiport pairs and demand distributed detailed in Section V.A, with flights being scheduled as soon as their trajectory was clear of conflicts. Table 2 contains the capacity results from the simulation. In most cases the simulated capacity is lower than the estimated capacity due to the effects of unequal demand, which causes a discrepancy between the number of desired flights along a route and the potential capacity of that route. The exceptions are the VP01-VP03 and VP01-VP05 trajectories, where the weighting allows a higher capacity through the angular intersection than the alternating case. Vertiport pair VP04-VP01 for instance, has the capacity for many more flights, but it simply does not have the demand for this higher capacity. VP05-VP01 has the opposite problem, because the demand is high enough that the capacity limit is nearly reached. This effect is also seen in the capacity for the entire airspace, where the simulated capacity was only 601 flights per hour, compared to the estimated capacity of 1324.

Starting Location	Ending Location	Route Defined?	Demand Percentage	Capacity (Estimated)	Capacity (Simulated)
VP01	VP03	Y	16%	92	123
VP01	VP05	Y	10%	58	71
VP02	VP01	N	12%	150	57
VP04	VP01	N	16%	600	101
VP04	VP03	N	12%	212	63
VP05	VP01	N	33%	212	186

Table 2 Breakdown of the demand for the example airspace scenario, including the starting and ending vertiports, the route definition, the demand weighting, the estimated capacity, and the simulated capacity.

VI. Summary and Conclusions

As both industry, government, and regulatory partners prepare for the rise of urban air mobility flights, it is important to ensure that the airspace be able to safely accommodate the growing demand. Because potential use cases include airport shuttle trips, local trips, and even commuting trips, if the ticket cost is low enough, the anticipated demand is likely to be focused on downtown areas, with operations concentrated in these areas. Designing airspace route structures and other features can enable efficient use of the airspace to best accommodate future demand.

This work included theoretical and simulated capacity estimations for different types of airspace route structures, including one directional routes, angular intersections, perpendicular intersections, diverging intersections, and rotary intersections. The analyses show that angular intersections, particularly large angles, have a significantly reduced capacity. Rotary intersections, if feasible, could prove to be useful for reducing delays, but care must be taken to ensure they are sized appropriately so the additional time flown due to the longer route does not outweigh the benefits. In cases where there is an idea of the demand, if one route has a particularly high demand relative to other routes, it is beneficial to not include that route in the rotary intersection. These results can be used to create guidelines for modifying or designing aircraft route structures to maximize capacity, as is shown in the companion paper[12].

An example airspace was also analyzed to demonstrate the ability to estimate the capacity theoretically and by simulation using representative demand. The capacity for a given vertiport pair is estimated by looking at the intersections along each trajectory, while the capacity for the airspace is estimated by summing the capacity of each of the possible vertiport pairs. Simulation results show that with an equal demand distribution, the maximum capacity is not achieved because some trajectories will have greater capacity than demand, while others have demand that outweighs their capacity.

In addition to the work to analyze and improve the capacity of realistic airspace scenarios presented in our companion paper, future work includes expanding the analysis to include horizontal and vertical conflict resolution, as well as the delayed start time resolution used in this work. This will enable additional capacity for a given airspace, with the eventual goal of being able to fully accommodate UML-4 estimated demand levels for a major metropolitan area.

Acknowledgments

This work was funded by the UAM Subproject of the Aeronautics Research Mission Directorate's ATM-X Project.

References

[1] Chan, W. N., Barmore, B., Kibler, J., Lee, P. U., O'Connor, N., Palopo, K., Thipphavong, D. P., and Zelinski, S., "Overview of NASA's ATM-X Project," *2018 Aviation Technology, Integration, and Operations Conference*, AIAA 2018-3363, American Institute of Aeronautics and Astronautics, Atlanta, Georgia, Jun 2018. doi:10.2514/6.2018-3363, URL https://arc.aiaa.org/doi/10.2514/6.2018-3363.

[2] Levitt, I., "ATM-X UAM Subproject Overview," , Dec 2020. URL https://ntrs.nasa.gov/citations/20210000102, presentation, Accessed 19 May 2022.

[3] Xue, M., "Design Analysis of Corridors-in-the-Sky," *AIAA Guidance, Navigation, and Control Conference*, AIAA 2009-5859, American Institute of Aeronautics and Astronautics, Chicago, Illinois, Aug 2009. doi:10.2514/6.2009-5859, URL https://arc.aiaa.org/doi/10.2514/6.2009-5859.

[4] Xue, M., and Zelinski, S., "Complexity Analysis of Traffic in Corridors-in-the-Sky," *10th AIAA Aviation Technology, Integration, and Operations (ATIO) Conference*, AIAA 2010-9112, American Institute of Aeronautics and Astronautics, Fort Worth, Texas, Sep 2010. doi:10.2514/6.2010-9112, URL https://arc.aiaa.org/doi/10.2514/6.2010-9112.

[5] Xue, M., and Zelinski, S., "Optimal Integration of Departures and Arrivals in Terminal Airspace," Vol. 37, No. 1, Jan 2014, pp. 207–213. doi:10.2514/1.60489, URL https://arc.aiaa.org/doi/10.2514/1.60489.

[6] Xue, M., and Rios, J., "Initial Study of An Effective Fast-time Simulation Platform for Unmanned Aircraft System Traffic Management," *17th AIAA Aviation Technology, Integration, and Operations Conference*, AIAA 2017-3073, American Institute of Aeronautics and Astronautics, Denver, Colorado, Jun 2017. doi:10.2514/6.2017-3073, URL https://arc.aiaa.org/doi/10.2514/6.2017-3073.

[7] Mueller, E. R., Kopardekar, P. H., and Goodrich, K. H., "Enabling Airspace Integration for High-Density On-Demand Mobility Operations," *17th AIAA Aviation Technology, Integration, and Operations Conference*, AIAA 2017-3086, American Institute of Aeronautics and Astronautics, Denver, Colorado, Jun 2017. doi:10.2514/6.2017-3086, URL https://arc.aiaa.org/doi/10.2514/6.2017-3086.

[8] Vascik, P. D., Cho, J., Bulusu, V., and Polishchuk, V., "Geometric Approach Towards Airspace Assessment for Emerging Operations," Vol. 28, No. 3, July 2020, pp. 124–133. doi:10.2514/1.D0183, URL https://arc.aiaa.org/doi/10.2514/1.D0183.

[9] Goodrich, K. H., and Theodore, C. R., "Description of the NASA Urban Air Mobility Maturity Level (UML) Scale," *AIAA Scitech 2021 Forum*, AIAA 2021-1627, American Institute of Aeronautics and Astronautics, VIRTUAL EVENT, Jan 2021. doi:10.2514/6.2021-1627, URL https://arc.aiaa.org/doi/10.2514/6.2021-1627.

[10] "UAM Vision Concept of Operations (ConOps): UAM Maturity Level (UML) 4," National Aeronautics and Space Administration, Dec 2020.

[11] Levitt, I., Phojanamongkolkij, N., Horn, A., and Witzberger, K., "UAM Reserach Roadmap Rev 1.2," NASA/TM-20220008917, Washington, D.C., Jun 2022. URL https://nari.arc.nasa.gov/uam-research-roadmap.

[12] Cummings, W. G., Denham, C. L., and Smith, J. C., "Effect of Airspace Characteristics on Urban Air Mobility Airspace Capacity," *AIAA SciTech 2023 Forum*, To be Published, American Institute of Aeronautics and Astronautics, National Harbor, MD, Jan 2023.

[13] Guerreiro, N. M., Butler, R. W., Maddalon, J. M., and Hagen, G. E., "Mission Planner Algorithm for Urban Air Mobility – Initial Performance Characterization," *AIAA Aviation 2019 Forum*, AIAA 2019-3626, American Institute of Aeronautics and Astronautics, Dallas, Texas, Jun 2019. doi:10.2514/6.2019-3626, URL https://arc.aiaa.org/doi/10.2514/6.2019-3626.